

CSIRO
Division of Fisheries and Oceanography

REPORT 105

***In vivo* Chlorophyll *a* Fluorescence
in the Vicinity of Warm-core Eddies
off the Coast of New South Wales
1. September 1978**

D. J. Tranter, R. R. Parker
and
D. J. Vaudrey

1979

COMMONWEALTH SCIENTIFIC AND INDUSTRIAL RESEARCH ORGANIZATION
DIVISION OF FISHERIES AND OCEANOGRAPHY
P.O. BOX 21, CRONULLA NSW 2230

Reprint 1051

National Library of Australia Cataloguing-in-Publication Entry

Tranter, D.J.

In vivo chlorophyll *a* fluorescence in the vicinity of
warm-core eddies off the coast of New South Wales.

1. September 1978

(Division of Fisheries and Oceanography report; 105)

Bibliography

ISBN 0 643 02206 6

1. Marine biology — New South Wales. 2. Chlorophyll. 3. Fluorescence.

I. Parker, R.R., joint author.

II. Vaudrey, D.J., joint author. III. Title. (Series: Commonwealth
Scientific and Industrial Research Organization. Division of Fisheries
and Oceanography. Report; 105)

574. 92'5'78

©CSIRO, 1979

Printed by CSIRO, Melbourne

IN VIVO CHLOROPHYLL *a* FLUORESCENCE IN THE VICINITY OF WARM-CORE EDDIES OFF THE COAST OF NEW SOUTH WALES

1. SEPTEMBER 1978

D.J. Tranter, R.R. Parker and D.J. Vaudrey

CSIRO Division of Fisheries and Oceanography
P.O. Box 21, Cronulla, NSW 2230

CSIRO Aust. Div. Fish. Oceanogr. Rep. 105 (1979)

Abstract

The warm-core eddies "E" and "F" off the coast of New South Wales, Australia, in September 1978 were areas of low surface *in vivo* chlorophyll *a* fluorescence, dominated by what appeared in preserved samples to be flagellates. Eddy "E" was bounded on the south by a frontal zone dominated by diatoms where *in vivo* chlorophyll *a* fluorescence increased fourfold. There was no apparent relationship with nitrate concentration but fluorescence was always low wherever there was a deep mixed layer, as in the eddies, suggesting that light, not nutrients, was limiting the size of the standing crop. Cell counts, biomass estimates and extractable chlorophyll data support *in vivo* fluorescence as an index of autotrophic biomass. Field trials demonstrated that ambient fluorescence (F_A) was approximately half the maximum recorded after photosynthesis inhibition (F_M). There was evidence of diel variation in surface waters, suggesting a midday depression of photosynthesis efficiency.

INTRODUCTION

Anti-cyclonic warm-core eddies may be compared with the high pressure cells which occur in atmospheric circulation. They have been observed off the east Australian coast since the late 1950's but the spatial resolution of the eddies was not adequate to determine their structure until more recently. They are now understood as lens-shaped pools of warm water extending in diameter up to 200 km, and in depth to 300 m or more (Andrews and Scully-Power 1976). Their dynamics have been followed by satellite-tracked buoys (Cresswell 1976; Cresswell and Wood 1977). It has been suggested that their formation is due to baroclinic instabilities producing a downward motion causing the eddy to close off from the East Australian Current (Nilsson *et al.* 1977).

Little is known about the biology of warm-core eddies off the East Australian coast; research until now has been directed at their physical and chemical properties. More is known about the biology of warm-core anti-cyclonic eddies of the N.W. Atlantic Gulf Stream which are at present the focus of a multi-disciplinary study by the Woods Hole Oceanographic Institution (Anon. 1977).

The following concept has been adopted as a working hypothesis for this biological study - The nutrients available within the eddy during its lifetime originate with the original tongue of water isolated from the East Australian Current, and these constantly diminish because of detrital fallout. The only other exchanges take place through faunal migration across the boundaries. In

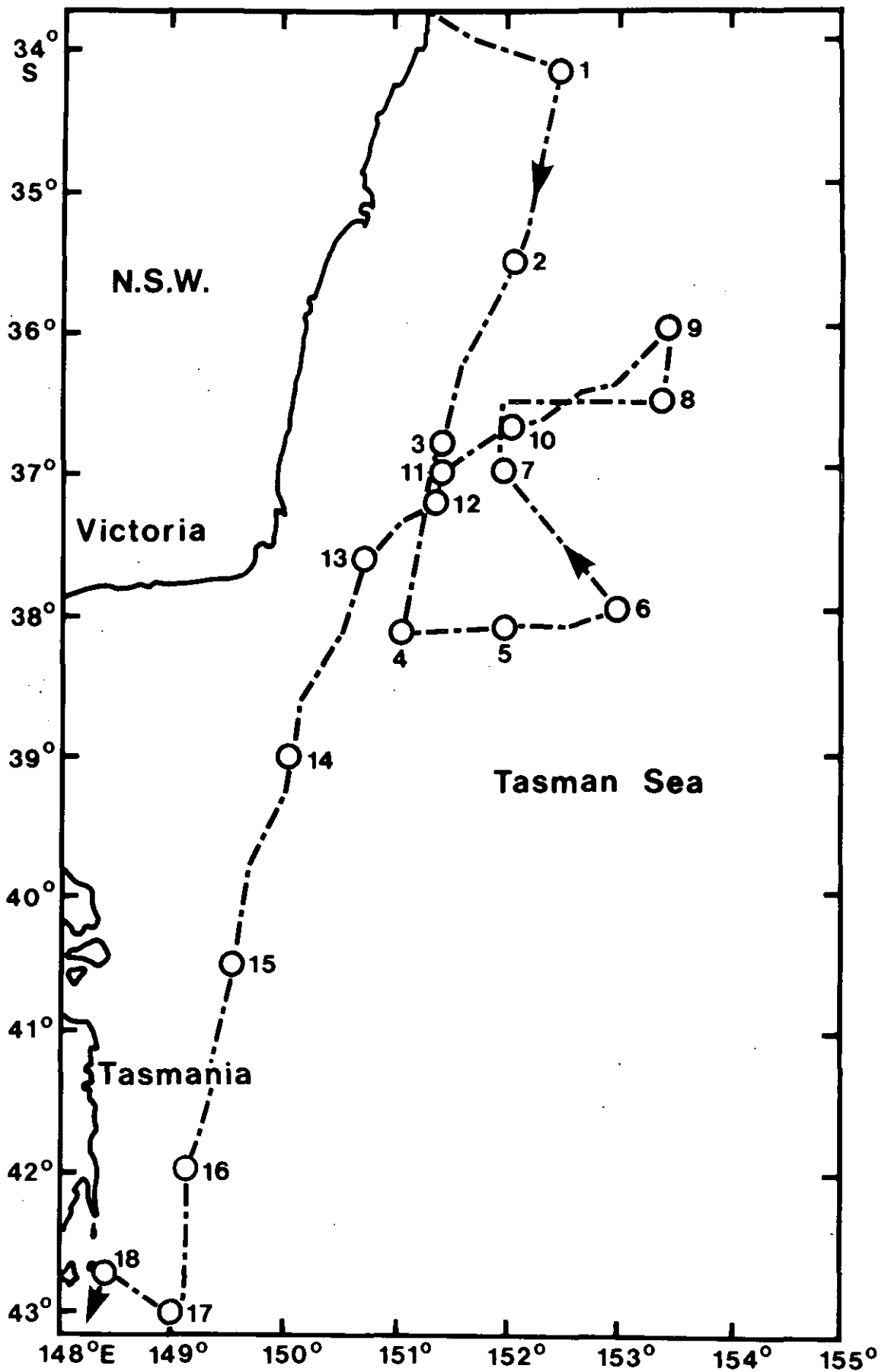


Fig. 1. Cruise track of "Sprightly", 15-22 September 1978 (SP12/78). Niskin bottle stations are indicated by open circles. (None at stations 2 and 5).

time, the water within the eddy becomes impoverished, while surrounding water is renewed through upwelling and coastal inputs. The food chain loses its primary production base and species composition changes. Eventually the whole biotic system runs down, until the eddy becomes a biological desert. This hypothesis may be tested by observing the dynamics of the autotrophic population within one or more eddies over their lifetime, a period of about 1-2 years.

Data presented in this report were obtained from *Sprightly* cruise 12/78 (15-22 September 1978) whose track is shown in Fig. 1 (Church 1978). It is the first step in testing the above hypothesis. The main research emphasis of the cruise was on the physical and chemical structure of an eddy (Eddy "E"), discovered on an earlier cruise (SP8/78) (Cresswell unpublished data). The work included continuous monitoring of surface salinity and temperature, sampling for surface nutrients in the region of the eddy, expendable bathythermograph profiles at 2-hourly intervals, and profiles for temperature, salinity, oxygen, silicate, nitrate and phosphate. The report which follows describes results based on *in vivo* chlorophyll *a* fluorescence with supporting and interpretative data from extractable chlorophyll pigment analyses and microscopic examination of the protoplankton.

Our primary purpose in this study is not to determine how much chlorophyll is present but how much phytoplankton - that is the standing crop. Because chlorophyll:carbon ratios vary by an order of magnitude (Banse 1977), extracted chlorophyll is no better an index of standing crop than *in vivo* chlorophyll fluorescence. The latter technique, on the other hand, has the capacity for generating rapid, continuous, real-time data that is the essence of ecological investigation in the field. Furthermore, the technique is more sensitive and can be adapted to measure not

only how much phytoplankton is present but also its efficiency in photosynthesis (Samuelsson and Öquist 1977), hence its potential rate of growth.

A short outline of the theoretical basis of *in vivo* chlorophyll fluorescence is given in the following section. This question will be dealt with in greater detail in a later paper.

METHODS

The principle of the *in vivo* chlorophyll fluorescence method (Lorenzen 1966) is as follows - Artificial light is modified by a low pass filter opaque to wavelengths longer than about 600 nm. This is used to excite chlorophyll *a* in the blue portion of the absorption spectrum, maximum in living diatoms and dinoflagellates at about 435 nm (Gaffron 1960, after Dutton and Manning 1941). Resulting fluorescence is measured through a narrow pass filter, opaque to wavelengths less than about 660 nm and greater than 710 nm, effectively isolating the red peak of *in vivo* fluorescence, maximum at about 695 nm (Govindjee and Govindjee 1974).

We have adopted, in our work, the following interpretation of *in vivo* chlorophyll *a* fluorescence: The capacity of the autotrophic population to absorb light quanta is indicated by the *in vivo* fluorescence of vital cells in which photochemistry is blocked (FM). This estimates phytoplankton biomass (Slovacek and Hannan 1977) but is subject to changes in absorption per unit pigment caused by conformational changes within the cell and within the chloroplasts, particularly in response to ambient light conditions (Mayer 1971; Kiefer 1973). There is also a "package effect" (Kirk 1975), small cells absorbing more light than large cells per unit of extractable pigment.

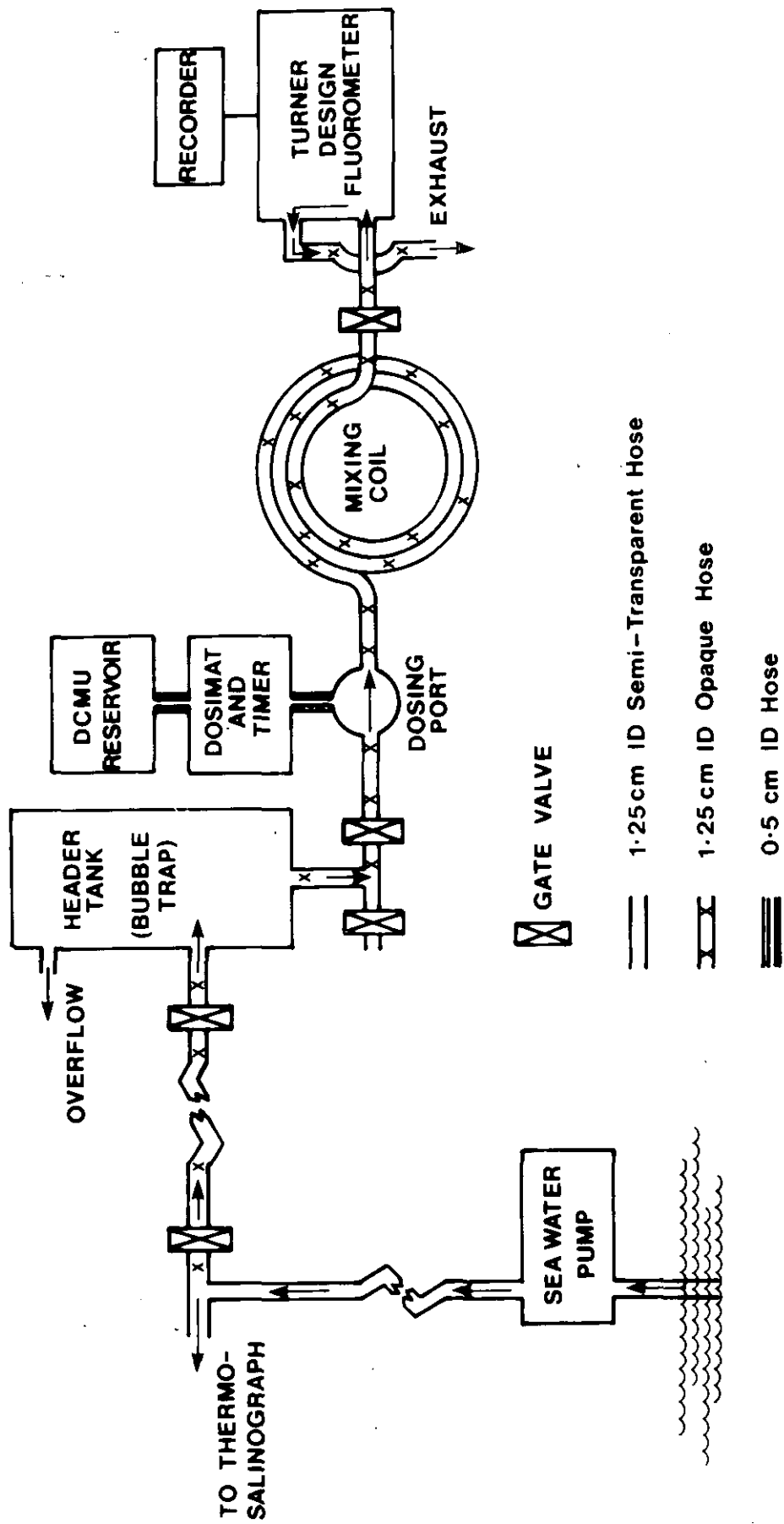


Fig. 2. Schematic of water supply for 'on stream' continuous flow fluorescence measurements.

The fraction of the absorbed quanta used in photosynthesis is an index to the relative growth rate of the autotrophic population (Samuelsson and Öquist 1977) specific to the instant of measurement. We term this fraction "photosynthetic quantum efficiency" (ϕ_p)

$$\phi_p = \frac{F_M - F_A}{F_M}$$

where F_A ("ambient fluorescence") is the fluorescence yield during photosynthesis. 'Ambient' conditions include not only those prevailing at the spot from which the sample was drawn but also subsequent conditions prior to measurement such as enclosure, transport (e.g. pumping), and storage. F_A may be thought of as a safety valve releasing absorbed quanta which cannot be used in photosynthesis. It is identified as

$$F_A = (1 - \phi_p) F_M \quad (2)$$

Both F_M and ϕ_p can vary, F_M as detailed above, and ϕ_p by environmental limitations, particularly nutrients (Slovacek and Hannan 1977).

The problem of control blanks is a difficult one and for our ocean work we have adopted distilled water which accounts for instrument zero error. Fluorescence emissions not under photosynthetic control, e.g. from leakage in the photosystem antennae, from altered chlorophyll pigments in dead cells and faecal pellets, and from free pigment molecules, are ignored at this stage of our knowledge. This assumption biases F_M in the direction of being too large and biases ϕ_p in the direction of being too small, i.e. the biomass is overestimated and the growth rate underestimated.

The types of fluorometer used in this survey were a Turner Design 10-005R Field Fluorometer (Turner Designs, 2247A Old Middlefield Way, Mountain View, California 94043, U.S.A.) for continuous monitoring of surface

fluorescence, used also for batch samples taken from the water column, and a Variosens II (Frügel and Koch 1976) fluorometer for *in situ* depth profiles.

The Variosens was lowered on a slip-ring hand winch to a depth of 100 m, with negligible wire angle, depth annotations being made on the chart record at 10 m intervals as read from a meter block. Speeds of lowering varied from 1 m sec^{-1} to 0.3 m sec^{-1} .

The Turner Design Fluorometer is a linear response instrument with a series of multiplicative ranges through which the fluorescent response may be recorded. These ranges change automatically due to electronic logic circuits within the instrument, with a manual override alternative. The instrument also has a blanking control, to adjust for residual fluorescence of the medium in which the chlorophyll is contained and a span adjustment to change the width of each range.

Standardization was carried out before and after the cruise with a piece of Corning glass filter, 3-69, which has a fluorescent response similar to chlorophyll *a* (Turner 1973), by using the span adjustment to generate a response of 70 units on the 3.16×100 scale (referred to here as "Turner units" or T.U.). The instrumental drift was less than 5% of full scale. The Variosens II was also standardised against 3-69 Corning glass. The quasi-logarithmic response of the instrument was linearised by means of a calibrated series of Schott Neutral Density Filters (Parker and Vaudrey, unpublished data), the units being referred to here as "Variosens units" or V.U. Intercalibration of these two instruments has not yet been carried out. Although "underway fluorescence" (pump samples), "on station fluorescence" (bottle samples), and "*in situ* fluorescence" (Variosens) are all measures of standing crop, they are not immediately comparable because of different ambient conditions.

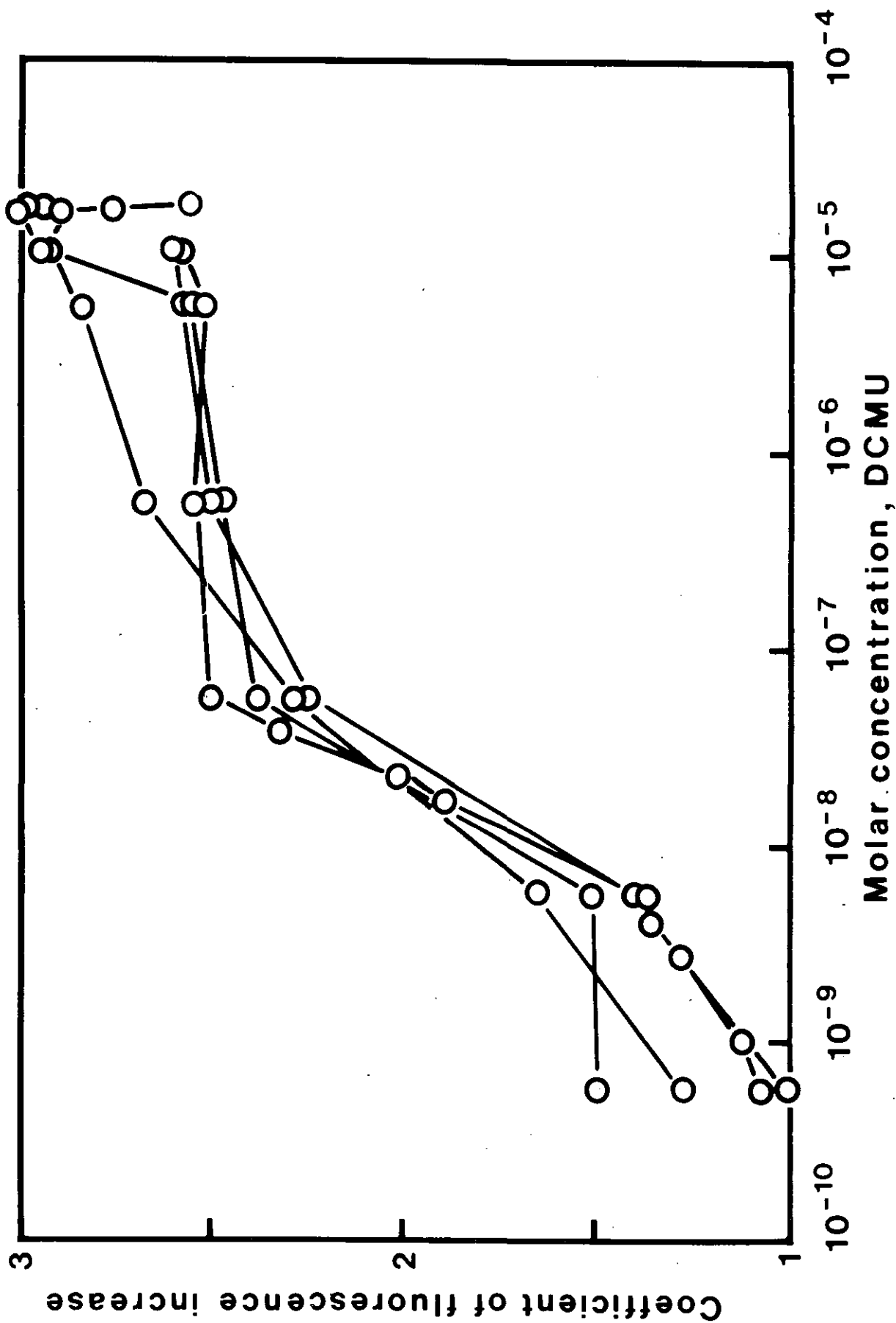


Fig. 3. Increase in fluorescence yield $\left\{ \frac{F_M}{F_A} \right\}$ induced by the photosynthesis inhibitor DCMU. Natural phytoplankton from Port Hacking was used. This figure shows that the dose required for maximum fluorescence response is of the order of 10^{-6} M.

Water for onstream continuous analyses was tapped from the ship's main pump, drawing its supply about 2 m below the surface (Fig. 2). From the seawater pump, water flowed through a 25 mm translucent polyethylene hose to a thermosalinograph, before which a T-piece and gate valve allowed part of the water to be piped through a 13 mm opaque "Nylex" (PVC) garden hose to the fluorometer. An 8 l header tank was installed to remove bubbles and provide a constant head of water for the fluorometer. From the header tank the flow passed by a dosing port through which a concentrated solution of DCMU (see below) was injected at periodic intervals. The water then passed through a 14 m vertical mixing coil of 1.25 cm internal diameter opaque hose to the fluorometer. The flow rate from the header tank to the fluorometer was approximately 3 l min^{-1} . The flow into the header tank from the seawater pump was greater than 5 l min^{-1} at all times. Consequently residence time in the header tank was less than 2 min and within the ship as a whole about 3 min. The residence time in the mixing coil downstream of the dosing port was 15 sec.

To measure F_M , the water continually flowing through the Turner Design Fluorometer was periodically dosed with DCMU (3-(3,4 dichlorophenyl)-1,1 dimethylurea), known also as "DIURON". DCMU blocks electron transport from photosystem II to photosystem I, eliminating the chemical conversion of absorbed light energy, thus maximizing the quantum fluorescence yield. The DCMU we used (Bayer Aust. Ltd.) was made up in saturated solution by heating (to 100°C) and stirring with distilled water, followed by filtration through Whatman GFC glass fibre filters. This concentrated solution was added to seawater to produce the desired concentration. The concentration producing the maximum response is of the order of 10^{-6} M (Fig. 3). In practice, we

used 1 ml of concentrate ($180 \mu\text{m}$) to approximately 30 ml of seawater. The time lag between dose and response is of the order of 10 sec (Fig. 4).

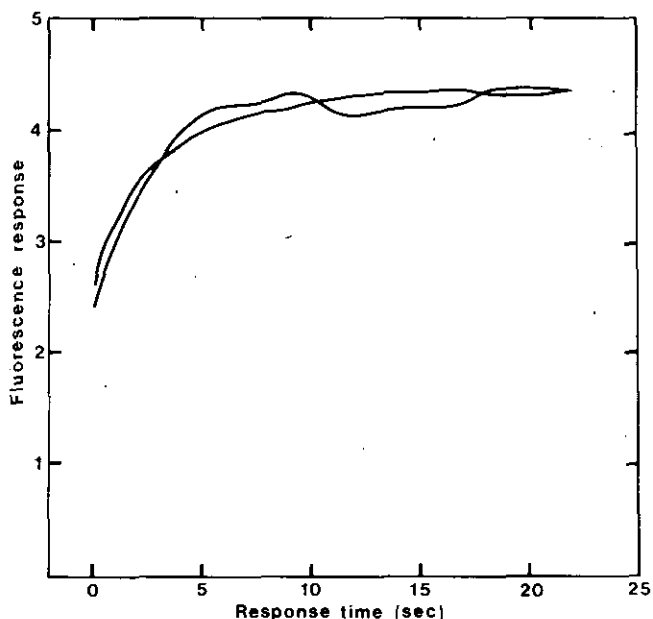


Fig. 4. Response/time curves induced by 10^{-5} Molar DCMU, natural phytoplankton from Port Hacking. Fluorescence values in arbitrary units. This figure shows that the time lag between dose and response is of the order of 10 secs.

Figure 5 shows a typical response (F_M), superimposed on the ambient level of fluorescence, F_A . This example is part of the continuous surface record, and was taken prior to Station 2 (Fig. 1). During this cruise, dosing was carried out automatically with the "DOSIMAT" [®] fitted with a timer delivering 50 ml of concentrate in 30 sec, thus providing the desired concentration. The dosed seawater then ran through the mixing coil, allowing time for inhibition before fluorescence was measured.

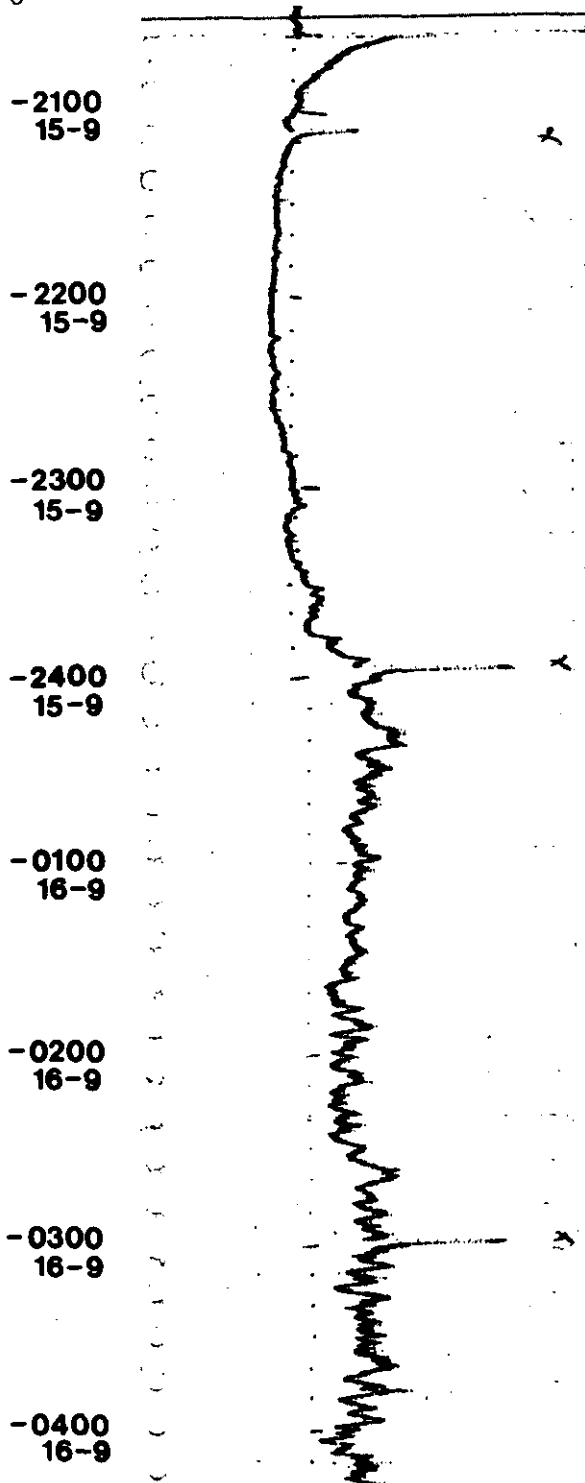


Fig. 5. Reproduction of a section of X, T fluorescence record from on-stream Turner Design fluorometer. Note the spikes induced by DCMU dosing at 3-hour intervals. SP12/78.

Samples for batch analysis were taken using 5 l Niskin bottles lowered to 75 m, 50 m, 25 m and surface on a near vertical wire ($<5^\circ$). From each Niskin bottle 200 ml were taken for taxonomic studies, 200 ml for fluorescence analysis (stored in dark bottles) and the remainder was filtered for chlorophyll analysis. The protocol for the analysis of batch samples was as follows:

- The cuvette was flushed with filtered seawater (FSW).
- The blank was determined.
- Ambient fluorescence (F_A) was determined.
- A duplicate aliquot was dosed with DCMU and a further reading taken (F_M).

Analyses were done under artificial light conditions which during the day were generally at lower illumination levels than those outdoors.

F_M was calibrated against chlorophyll a determined by the acetone extraction method. The fluorescence blanks were filtered seawater (FSW). Samples for chlorophyll analyses were filtered using GFC filters and a partial vacuum of less than 100 mm Hg. The filters were stored in the dark and frozen for three weeks prior to their analysis. Pigments were extracted in 100% acetone and absorption values determined for pigments in 90% acetone using a Zeiss PM4 Spectrophotometer. Concentrations were calculated according to the trichromatic equations of Jeffrey and Humphrey (1975) for mixed phytoplankton. Coefficients of determination of linear regressions between fluorescence and chlorophyll were calculated by the Cornish method as used by Black and Griffiths (1975), i.e.

$$R_l^2 = 1 - \frac{\sum (Y_i - \hat{Y}_i)^2}{\sum (Y_i - \bar{Y})^2}$$

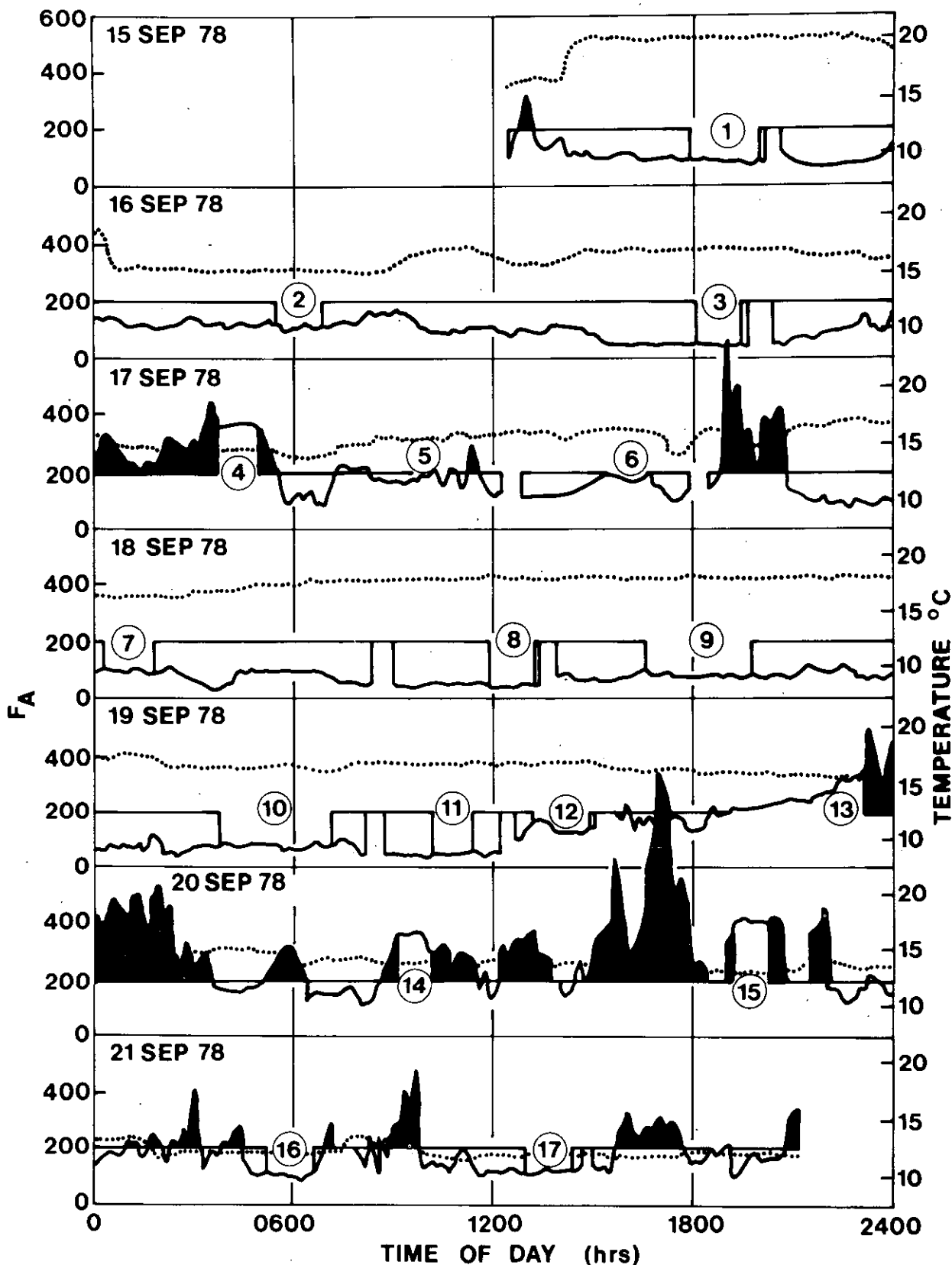


Fig. 6. Record of F_A and surface temperature for SP12/78. Breaks indicate vessel on station when the fluorometer was used in batch mode for station profiles. Values higher than 200 TU (the reference line) are black to indicate areas of high biomass. See Fig. 7 and 8 for station positions relative to eddies.

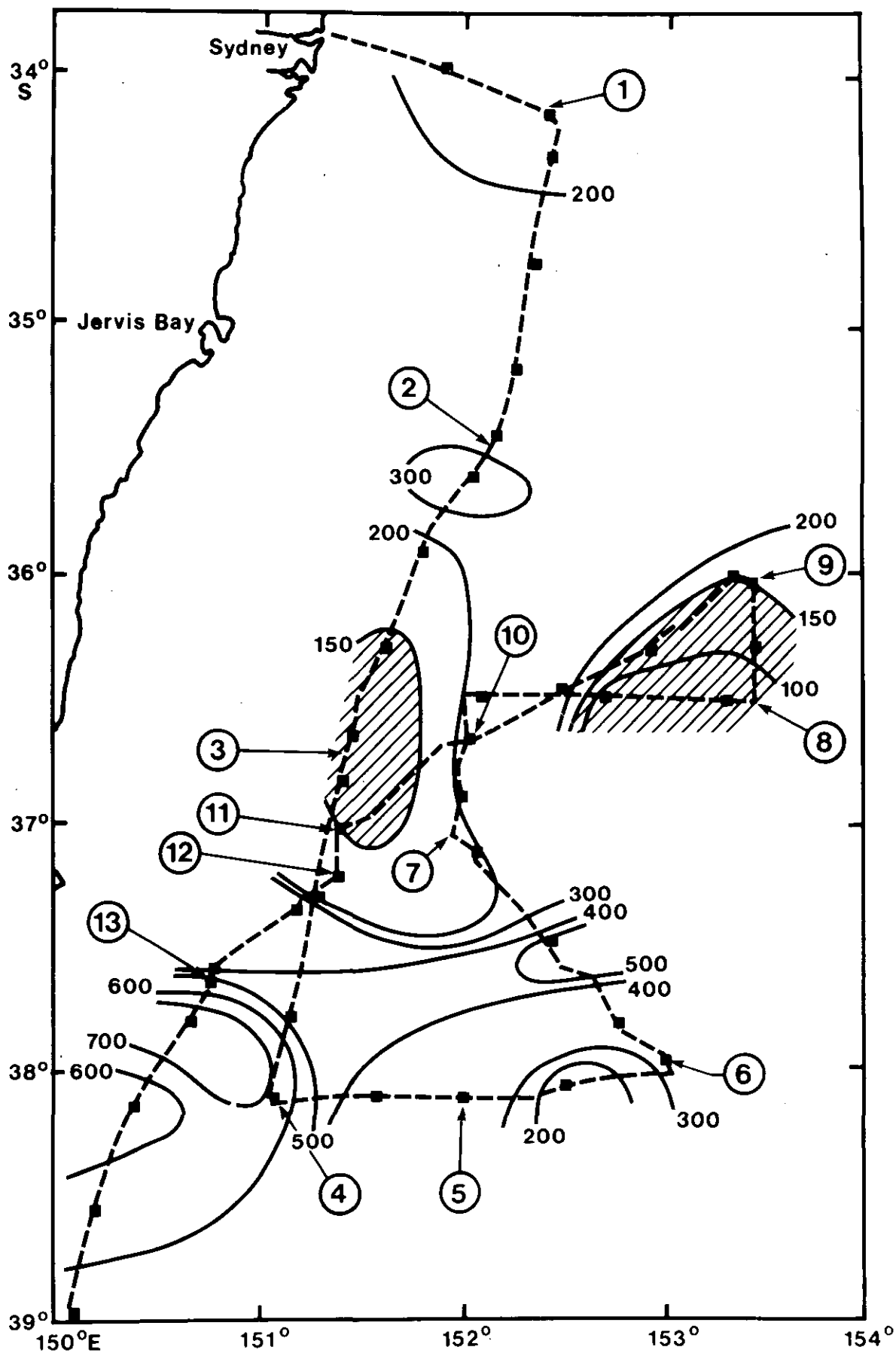


Fig. 7. Distribution of surface fluorescence (F_M) in the study area. Isopleths are drawn at 100, 150, 200, 300, etc. TU. Areas of low biomass are emphasized by hatching. These conform rather closely to the positions of the eddies shown in Fig. 8. Vertical profile stations are shown by circled numbers.

where R_j^2 is the coefficient of determination modified for a regression, constrained through the origin 0,0, Y_i is the estimated value corresponding to the i th observation Y_i , and $\bar{Y} = \frac{1}{n} \sum Y_i$.

The 200 ml samples for taxonomic study were fixed with iodine solution and stored in dark bottles for laboratory analysis. The samples were then settled and examined using the Uttermohl inverted microscope technique for quantitative estimates (Lund *et al.* 1958). Cells were first classified according to broad taxonomic groups: diatoms, flagellates, dinoflagellates and ciliates. Diatoms and dinoflagellates were further subdivided into genera, and dinoflagellate aplanospores (non-motile encystments) were noted separately. The "flagellates" category was a catch-all for cells not recognized otherwise. There is little doubt that true flagellates were included, but with the iodine treatment the flagella could seldom be recognized and body form was changed from that observed in fresh material. It was also not possible to distinguish autotrophic from heterotrophic forms. All taxa were further subdivided according to size. The cells were measured as either spheres (diameter) or cylinders (diameter and length) and biomass was estimated from calculated volumes assuming a specific density of 1.0. The cells of given volumes were then classified according to Sheldon-Parsons (1967) size groups of ascending doublings of volume. The counting/sizing protocol was to count abundant organisms (usually the small, round 5 μ diameter, flagellates), until a total of 400 of the most abundant kind/size category was reached, and to note the fraction of the entire field counted. Counting for the larger but scarcer items was continued until either the most abundant class/size group reached 400, or the entire sample had been counted. These counts were then standardized to a per litre basis.

RESULTS

The distribution of surface F_A along the cruise track is shown in Fig. 6 together with the temperature record. A reciprocal relationship was often observed between these two parameters, particularly in frontal regions. The distribution of F_M is shown in Fig. 7. This closely describes the location and extent of the eddies "E" and "F" as determined by temperature isopleths at 250 m (Fig. 8).

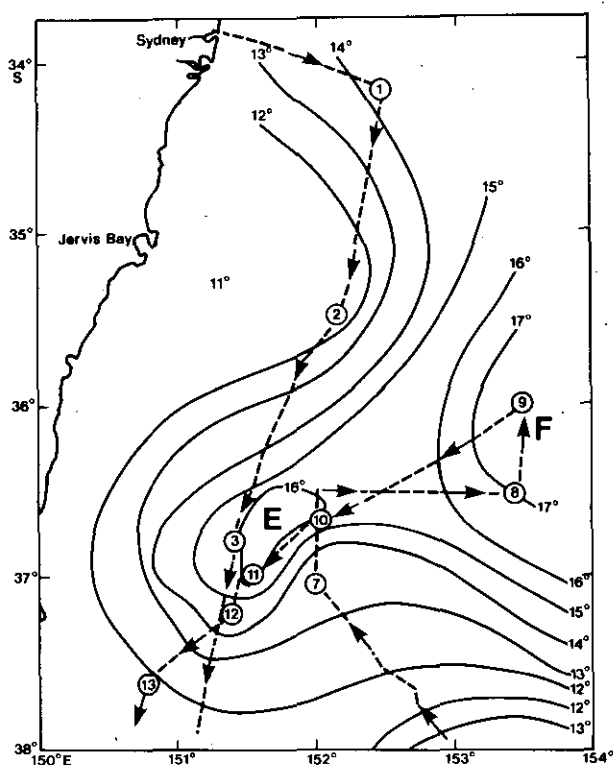


Fig. 8. Isopleths of temperature at 250 m determined by XBT. Source: Church, J. (M.S.) Cruise Report for SP12/78. Vertical profile stations are shown by circled numbers.

The centres of the eddies, characterized by *in vivo* fluorescence minima ($F_M < 150$ TU), were located at about $36^{\circ}45'S$, $151^{\circ}30'E$ and $36^{\circ}30'S$, $153^{\circ}E$. Eddy "E" was bounded on its southern margins by a relatively narrow zone of rapidly increasing F_M accompanied by a sharp decrease in surface temperature.

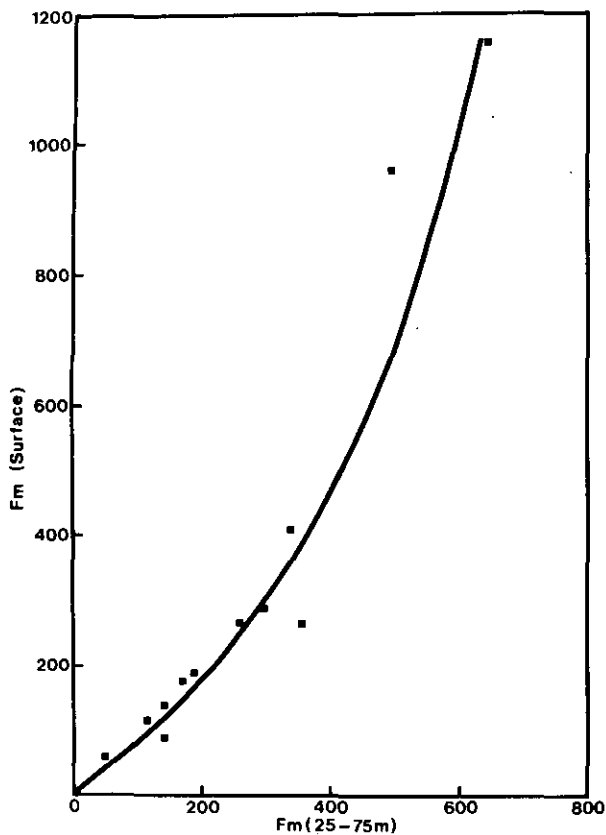


Fig. 9. Relationship between surface and subsurface fluorescence. Here, surface observations are an approximate index of average phytoplankton concentration in the 75 m water column beneath.

Figure 9 shows the relationship between surface and subsurface (25-75 m) fluorescence based on Niskin samples. On this cruise, perhaps because of winter mixing, surface properties are an index of properties in the water column beneath. Fluorescence records underway and ocean color observations from satellite may therefore be used with greater confidence.

The vertical distribution of F_A was measured *in situ* at several stations within and without the two eddies. Progressive difficulty was met with equipment used with the Variosens for obtaining vertical profiles of F_A . Results considered reliable were obtained at Stations 1-4 and 6-9 and are shown in Table 1. Values given in the last row are integrated for

the water column from 0 to 100 m and represent a biomass estimate comparable among stations. Stations 3, 7 and 8 had the lowest biomass and were associated with the eddies defined by T_{250} (Fig. 8). Station 7 which was exceptionally low lay near the southeast edge of eddy "E". The outstanding feature of the data set is the high *in vivo* fluorescence (F_A) at Station 4.

Although F_A appeared to indicate spatial variation in phytoplankton concentration to the extent that it defined the boundaries and geometry of two warm-core eddies (Figs 6, 8), there was also a suggestion of a diurnal component. This is evident in the distribution of ϕ_p (Fig. 10).

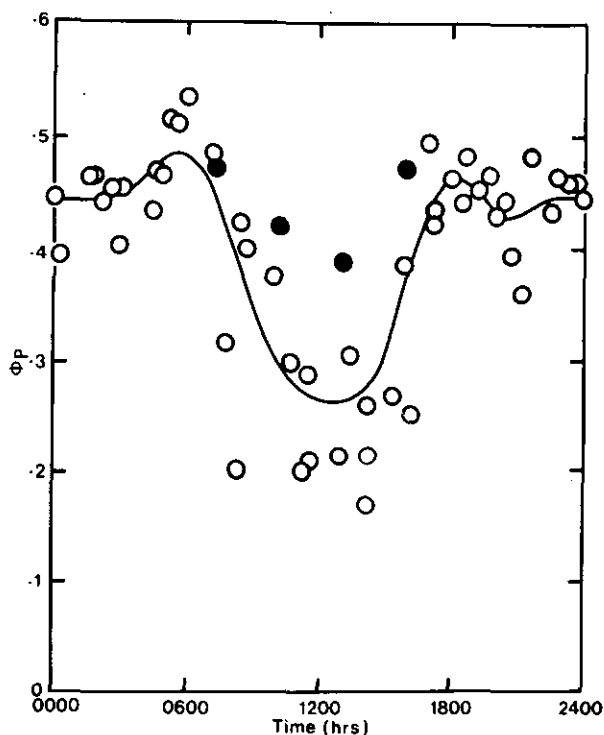


Fig. 10. Diel pattern of photosynthetic efficiency (ϕ_p), surface on-stream data only. ϕ_p is low at noon. Note 4 solid circles for data obtained under overcast conditions. All data were averaged within 3-hour time cells as shown by \circ . The faired line connecting these points was used to correct the data for diel trend, thus reducing the relative standard deviation by 20%.

For the greater part of the day, ϕ_p was between 0.4 and 0.5. However, it frequently declined at noon to 0.3, or even 0.2. Among the daytime data points are a set of four, arising from observations on a day (19 September) when the weather changed at about 1000 to overcast and rainy. ϕ_p , which appeared early on to be declining with the general trend, then deviated noticeably, maintaining higher than normal values throughout the midday hours. This suggests that a possible midday photoinhibition of surface samples should be looked for. The surface pattern was not observed subsurface (Fig. 11).

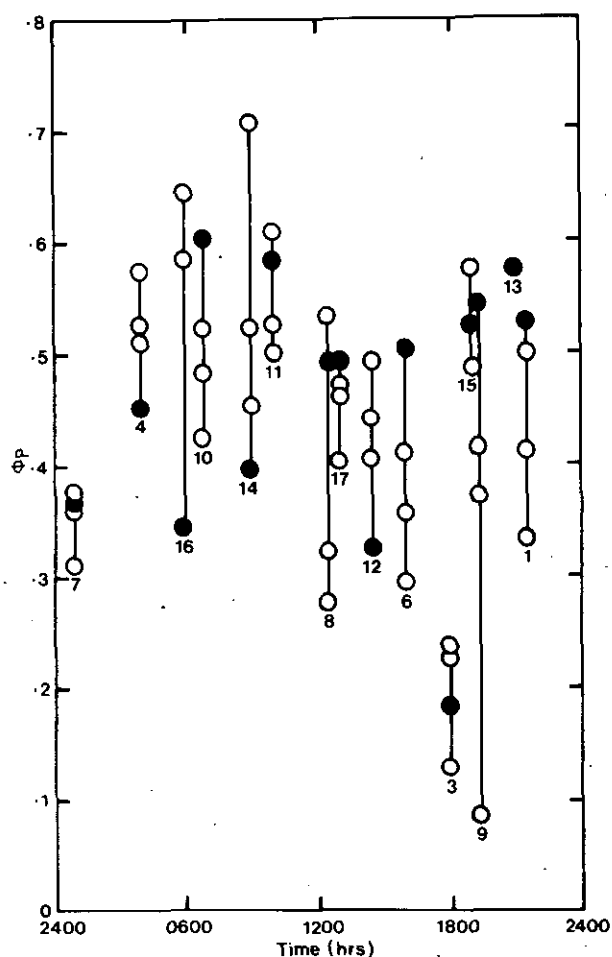


Fig. 11. Diel pattern of photosynthetic quantum efficiency (ϕ_p) for Niskin bottle samples taken at 0 m (solid circles), 25, 50 and 75 m depths. Values for each station identified by number are connected by a vertical line. Total number of samples available = 55.

In this data array, the relatively large variance obscured any definite relationship. However, we wish to emphasize that samples taken by water bottle and stored for up to an hour before analysis are not comparable with samples taken underway and analysed within a few minutes of collection.

ϕ_p data were averaged within 3-hour time cells and these points connected with a faired line which was used to correct the data set for diel trend. This treatment reduced the relative standard deviation by 20%. The corrected values are plotted in Fig. 12.

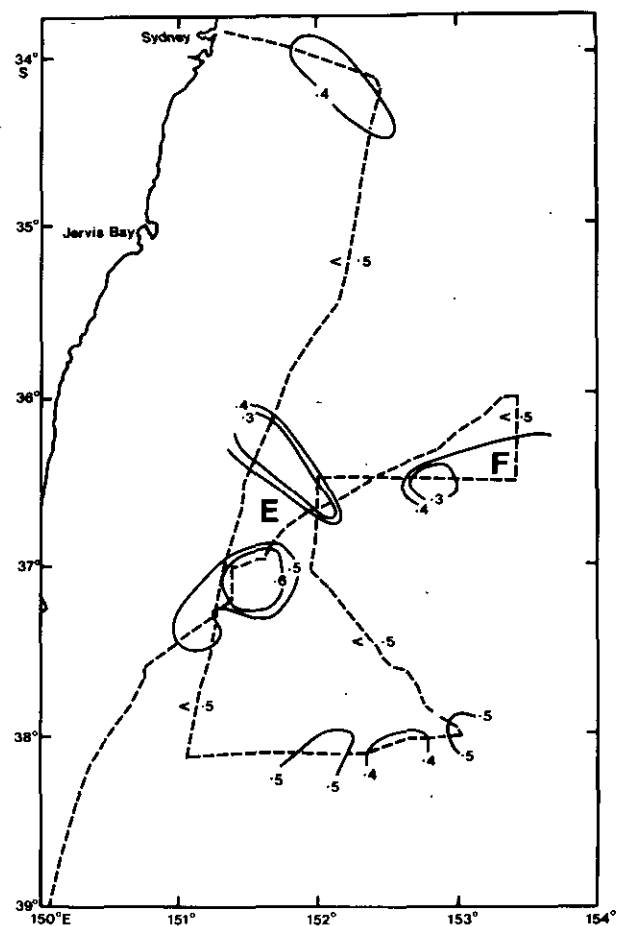


Fig. 12. Distribution of surface ϕ_p in the study area. Isopleths are drawn at 0.3, 0.4, 0.5 and 0.6. ϕ_p is generally low in eddy areas except for the SW portion of eddy "E".

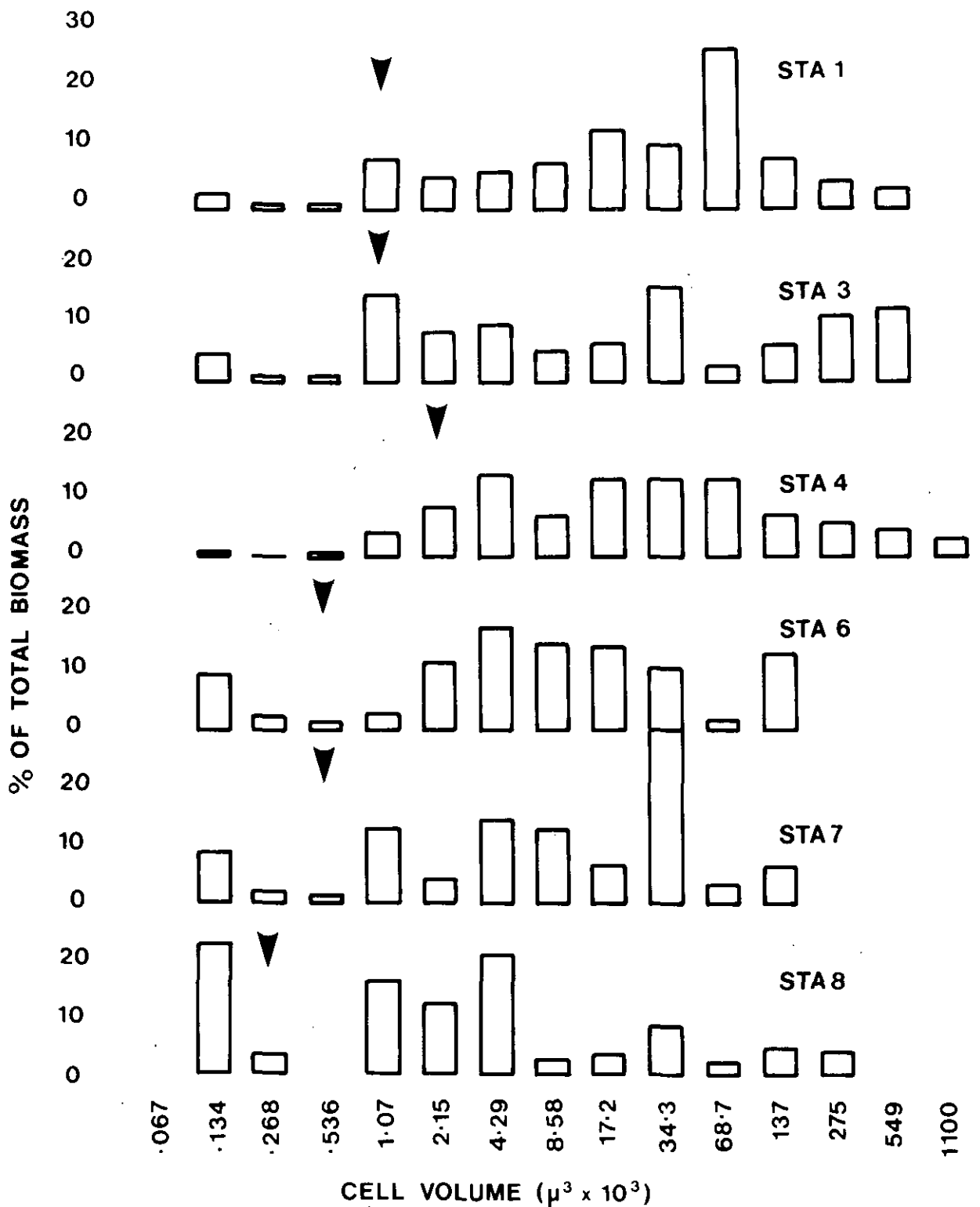
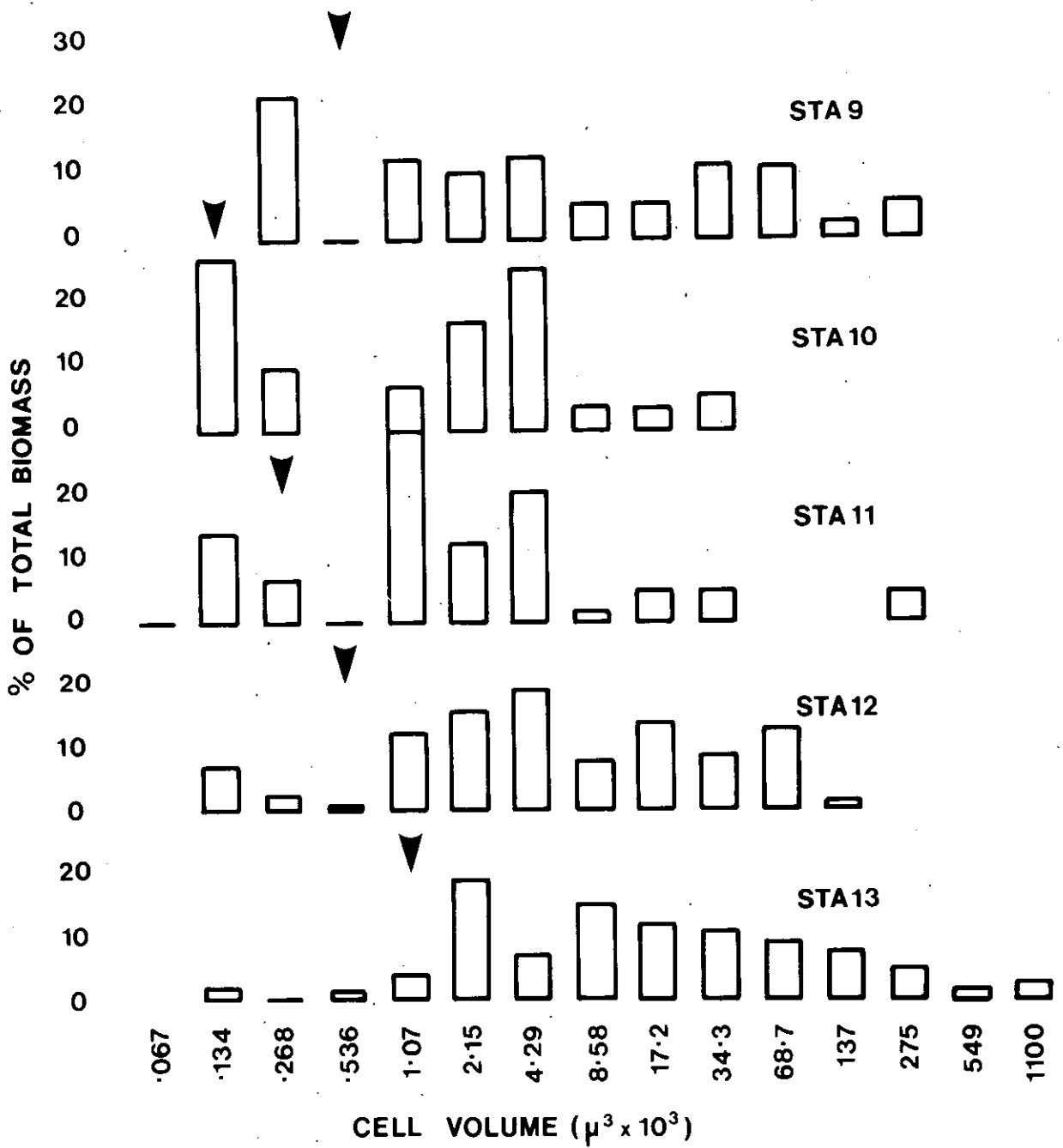


Fig. 14. Comparison of size distributions (Sheldon-Parsons size groups) of protoplankton among surface water samples. The group in which the average size ($\Sigma \text{biomass} / \Sigma \text{number}$) would fall is indicated by an arrow. Stations 9-13, SP12/78. The figure shows that stations outside the eddies (such as 1, 4 and 13) generally had larger phytoplankton cells than eddy stations (such as 8, 10 and 11).

Fig. 14 (contd).



The isopleths suggest that the phytoplankton of eddy "F" was characterized by a relatively low ϕ_p , whereas in eddy "E" ϕ_p was relatively high in the southern part and relatively low in the northern part. It is interesting that the northern part of eddy "E" had low F_M (Fig. 7) and low ϕ_p , whereas the southern part had low F_M and high ϕ_p . Another area of low F_M and low ϕ_p was located at about 38°S , $152^\circ30'\text{E}$, coincident with a T_{250} rise of more than 1°C , perhaps the edge of another eddy.

The relationship between fluorescence and extractable chlorophyll a for the Niskin bottle samples is shown in Fig. 13. Chlorophyll a was predictable by F_M ($\text{chl } a = 2.370 \times 10^{-3} F_M$, $R^2 = 0.75$, $N = 55$).

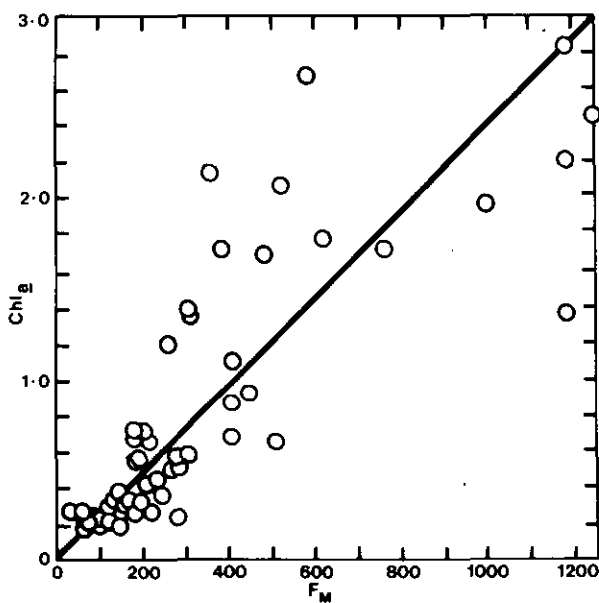


Fig. 13. Regression of extracted chlorophyll a on F_M fitted through 0,0. Niskin bottle samples (as in Fig. 11) 0-75 m, all available stations SP12/78. ($\text{chl } a = 2.370 \times 10^{-3} F_M$, $R^2 = 0.75$, $N = 55$).

Estimates of protoplankton biomass (as $\mu\text{g } \ell^{-1}$ derived from micro-measurements) for surface samples

from Stations 1, 3, 4, 6, 7, 8, 9, 10, 11, 12 and 13 are given in Appendices 1-11. Although the method is crude, several differences among the stations are evident, e.g. organisms tended to be smaller in eddy regions than either north or south (Fig. 14). Differences in taxonomic composition (major protoplankton groups) are set out in Table 2. Total biomass was relatively low within the two eddies but increased rapidly away from the core and dramatically so at the cold water front to the south (Stn 4, 13). Diatoms were relatively sparse in the eddy region (e.g. Stn 3, 8) and dominant in areas of high biomass. Within the eddy areas, flagellates formed the largest portion of the biomass. The complete "taxonomic" classification (genera and size/shape) is summarised in Table 3. It is evident from this comparison that biomass is directly related to the number of taxonomic units, i.e. the larger the biomass the larger the number of different "kinds" of protoplankton. There was a tendency for dinoflagellates (including aplanospores) to be relatively more important in the southern colder water.

A further comparison is made in Fig. 15 of biomass and $\text{chl } a$ as functions of F_M . Biomass is obviously biased when estimated by a fitted regression passing through 0,0. At low values of F_M the biomass is underestimated, at high values of F_M the biomass is overestimated. This bias may result from the "package" effect of cell size on fluorescence. When the total amount of pigment is held constant in a suspension of cells, more light will be absorbed (and fluoresced) if the cells are smaller (Kirk 1975). The data points for $\text{chl } a = a F_M$ suggest curvature in the opposite direction, e.g. at low values of F_M , $\text{chl } a$ is overestimated and at high values of F_M , $\text{chl } a$ is underestimated.

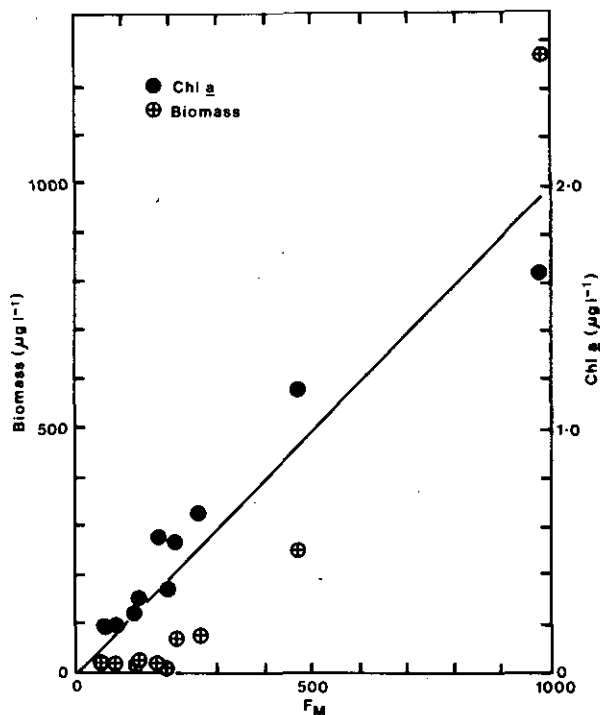


Fig. 15. Comparisons of biomass and extracted chlorophyll *a* as linear functions of F_M . Regression fitted through 0,0. Scales are adjusted so that fitted regression lines are shown by the solid diagonal line for both regressions.

(Biomass = $1.024 F_M$, $R^2 = 0.80$;
chl *a* = $1.182 \times 10^{-3} F_M$, $R^2 = 0.82$).

DISCUSSION

This first survey of *in vivo* chlorophyll *a* fluorescence of warm-core eddies off the N.S.W. coast suggests that Eddies "E" and "F" were waters of relatively low protoplankton standing crop. The possibility exists that they are detectable from the air on the basis of their colour, perhaps by satellites monitoring ocean colour such as the Coastal Zone Colour Scanner (Hovis 1975). The strong fluorescence front on the southern edge of eddy "E" (Fig. 7) is a source of special interest. This front reflects the likely presence of a cooler southern water mass contiguous with the eddy. At other times of the

year the margins of warm-core eddies off the coast may well abut on warmer and/or poorer water masses.

The principal question posed by the September pattern of *in vivo* chlorophyll fluorescence is why phytoplankton was sparser in the eddies than in the surrounding sea. In general, phytoplankton production is mainly limited by either nutrients or light. Within the eddies, nitrate was usually in excess of $2 \mu\text{g-at } \ell^{-1}$ and fairly evenly distributed through the water column (Fig. 16).

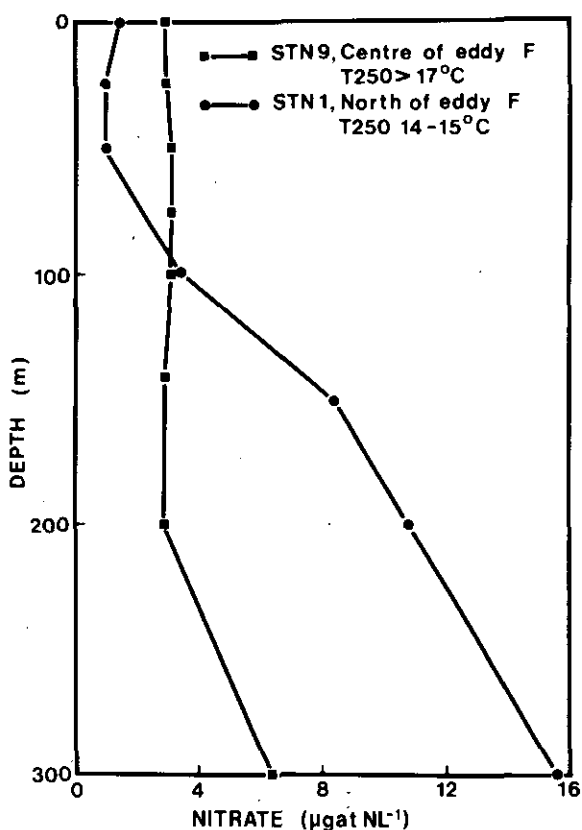
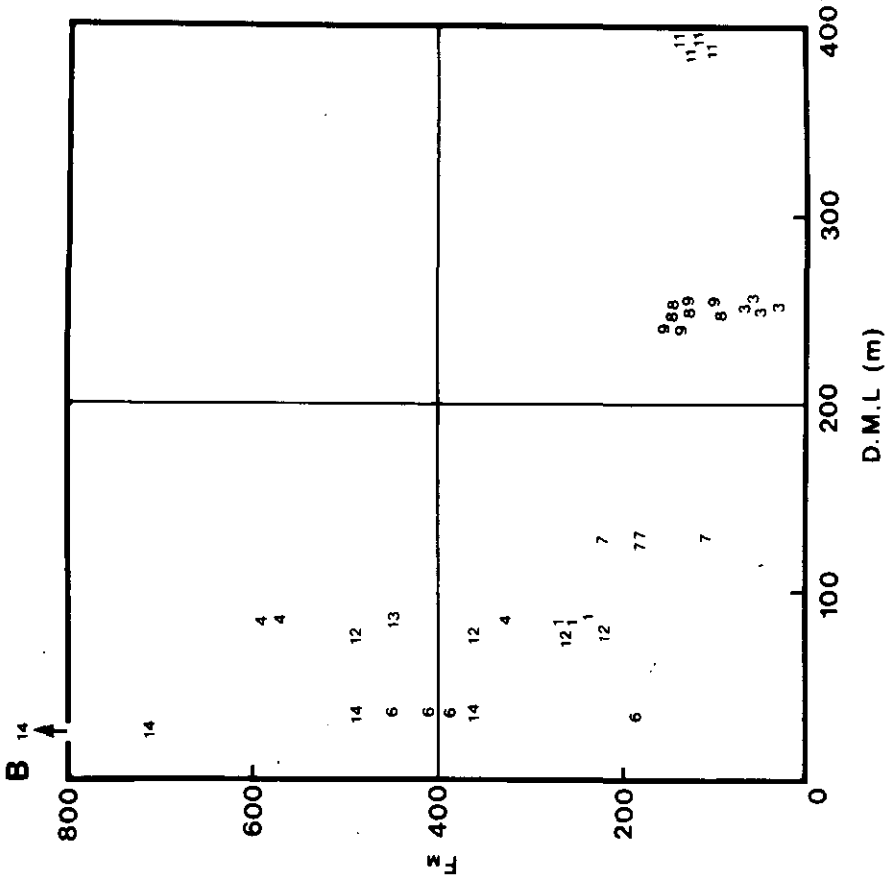
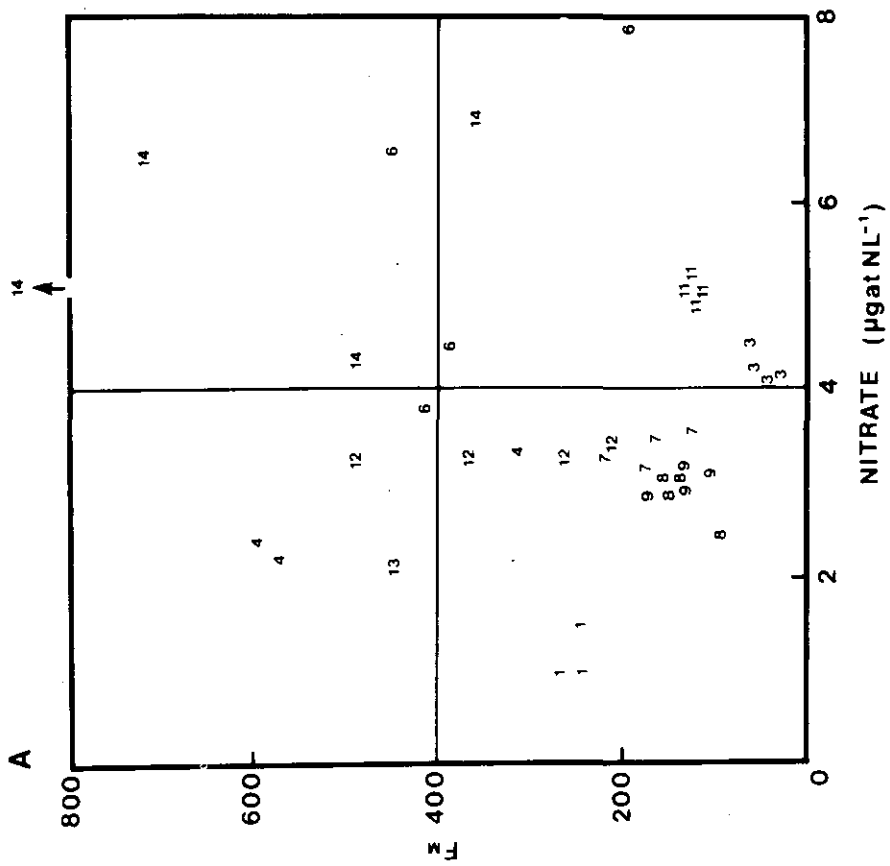


Fig. 16. Depth profiles of nitrate concentration inside and outside eddy "F". Within the eddy, nitrate is more uniform with depth and more than $2 \mu\text{g-at } \ell^{-1}$.

Outside the eddies, there was less nitrate above 100 m and more below. Neither standing crop (F_M) nor growth rate (ϕ_p) bore much relationship to nitrate (Fig. 17).



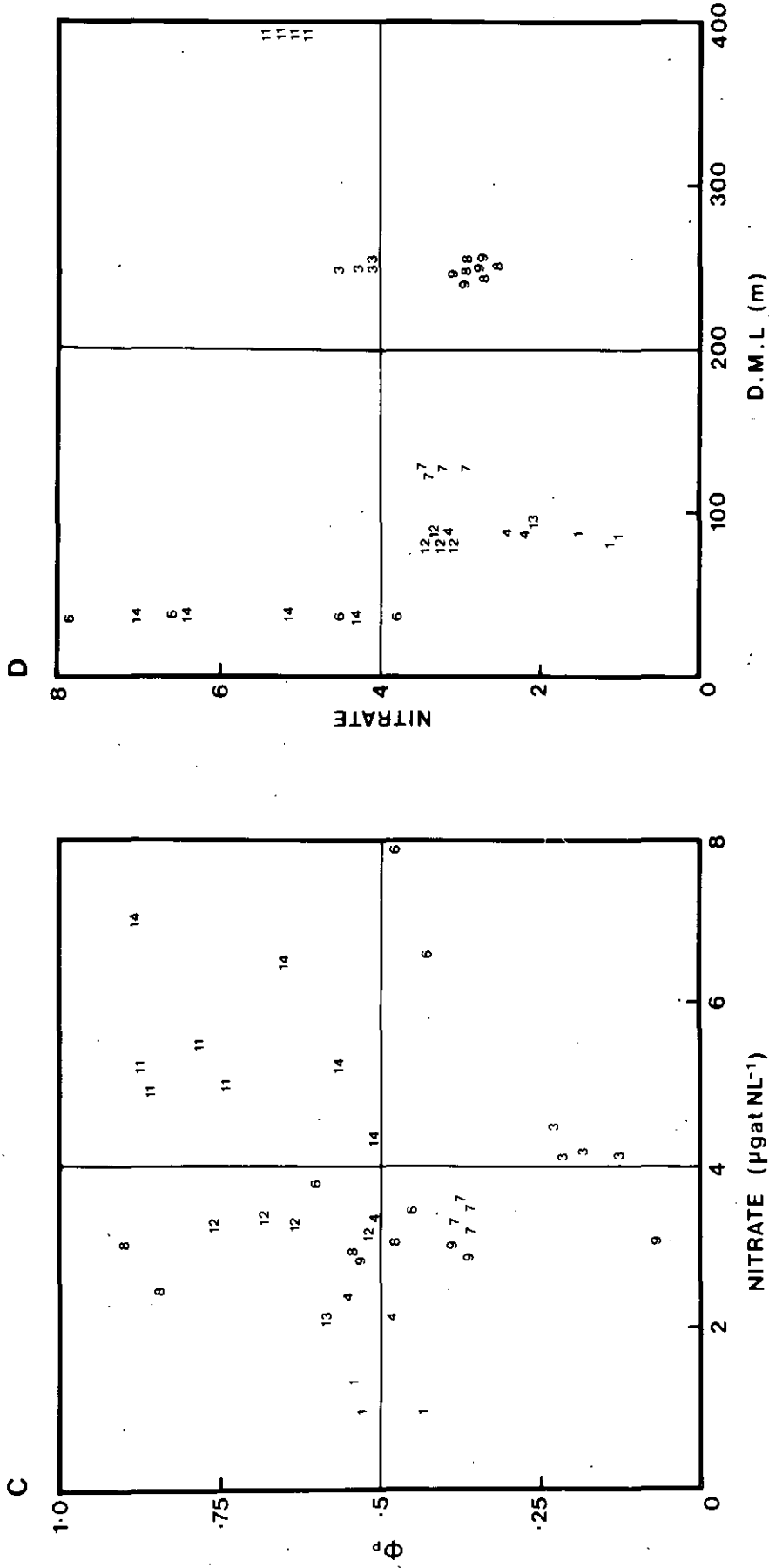


Fig. 17. Relationship between (A) F_M and Nitrate, (B) F_M and depth of the mixed layer, (C) ϕ_p and Nitrate, (D) Nitrate and DML. The numbers plotted are the stations shown in Fig. 1, 7 and 8, Niskin samples from 0, 25, 50 and 75 m. Stns 1, 4 and 13 have missing samples. The figure shows that neither standing crop (F_M) nor growth rate (ϕ_p) had any apparent relationship with nitrate but wherever there was a deep mixed layer there was a low standing crop.

However, wherever there was a deep mixed layer, as in the eddies, the standing crop was low. This suggests that phytoplankton production in September was limited by light, not nutrients (Sverdrup 1953).

The predominance of "flagellates" within the eddies at this time when the water column was isothermal to 250 m may be significant. It will be interesting to follow events in the oceanic spring when the eddies develop a shallow thermocline.

The increase in fluorescence yield obtained by inhibiting photosynthesis with DCMU was usually as spectacular as Slovacek and Hannan (1977) have described. Their experience was that the use of this technique would reduce the variability of fluorescence/chlorophyll *a* ratios by increasing the fluorescence yield to a maximum. However, our results suggest several problems, such as the effects of cell size, life cycle and conformation and distribution of chloroplasts on absorption, which need to be investigated further.

ACKNOWLEDGMENTS

Mrs R. Campbell carried out the chlorophyll analyses and the preliminary tests on photosynthesis inhibition. Thanks are due to the Electronics staff of this laboratory for the maintenance of the fluorimeters and to the workshop for other gear and equipment. Mr L. Rea assisted with cruise preparations and carried out the microscopic examinations and measurements of the protoplankton. The Captain and crew of *Sprightly* provided enthusiastic and welcome support at sea. Figure 8, describing the geometry of the eddy on the basis of the temperature at 250 m, was kindly made available by the Cruise Leader of SP12/78, Mr John Church. Mr Denis Reid, Division of Mathematics and Statistics, was consulted on the statistical interpretations.

REFERENCES

- Andrews, J.C., and Scully-Power, P. (1976). The structure of an East Australian Current anticyclonic eddy. *J. Phys. Oceanogr.* 6, 756-765.
- Anon. (1977). Interdisciplinary Workshop on Gulf Stream Anticyclonic Eddies, *Woods Hole, 1977*. Oceanographic study of warm core Gulf Stream rings and the north-west Atlantic slope water region: report and proceedings. p.110. (Woods Hole Oceanographic Institution: Woods Hole).
- Banse, K. (1977). Determining the carbon-to-chlorophyll ratio of natural phytoplankton. *Mar. Biol.* 41, 199-212.
- Black, J.L., and Griffiths, D.A. (1975). Effects of live weight and energy intake on nitrogen balance and total N requirement of lambs. *Br. J. Nutr.* 33, 399-413.
- Church, J. (1978). Cruise Summary R.V. "Sprightly" Cruise 12/78. Mimeo. CSIRO Aust. Div. Fish. Oceanogr., Cronulla.
- Cresswell, G.R. (1976). A drifting buoy tracked by satellite in the Tasman Sea. *Aust. J. Mar. Freshwater Res.* 27, 251-62.
- Cresswell, G.R., and Wood, J.E. (1977). Satellite tracked buoy data report II. Tasman Sea releases November 1976-July 1977. CSIRO Aust. Div. Fish. Oceanogr. Rep. 91.
- Früangel, F., and Koch, C. (1976). Practical experience with Variosens equipment in measuring chlorophyll concentrations and fluorescent tracer substances, like Rhodamine, Fluorescein and some new substances. *I.E.E.E. J. Oceanic Eng.* 1(1), 21-32.
- Gaffron, H. (1960). Energy storage: photosynthesis. In 'Plant Physiology'. (Ed. F.C. Stewart). pp. 3-277. (Academic Press: London).
- Govindjee, and Govindjee, R. (1974). The absorption of light in photosynthesis. *Sc. Amer.* 231(6), 68-82.

- Herman, A.W. (1975). Chlorophyll and dye detection with the Variosens fluorometer. Bedford Institute Report Series/BI-R 75-2, 1-32.
- Hovis, W. (1975). The Nimbus G. Coastal Zone Color Scanner. (NASA: Washington, D.C.). Unpublished manuscript.
- Jeffrey, S.W., and Humphrey, G.F. (1975). New spectrophotometric equations for determining chlorophylls *a*, *b*, *c*₁ and *c*₂ in higher plants, algae and natural phytoplankton. *Biochem. Physiol. Pflanz.* 167, 191-194.
- Kiefer, D.A. (1973). Chlorophyll *a* fluorescence in marine centric diatoms: Responses of chloroplasts to light and nutrient stress. *Mar. Biol.* 23, 39-46.
- Kirk, J.T.O. (1975). A theoretical analysis of the contribution of algal cells to the attenuation of light within natural waters. *New Phytol.* 75, 11-20.
- Lorenzen, C.J. (1966). A method for the continuous measurement of *in vivo* chlorophyll concentration. *Deep-Sea Res.* 13, 223-227.
- Lund, J.W.G., Kipling, C., and LeCren, E.D. (1958). The inverted microscope method of estimating algal numbers and the statistical basis of estimations by counting. *Hydrobiologia* 12, 143-170.
- Mayer, F. (1971). Light-induced chlorophyll contraction and movement. In 'Structure and Function of Chloroplasts'. (Ed. Martin Gibbs). p.286. (Springer-Verlag: Berlin).
- Nilsson, C.S., Andrews, J.C., and Scully-Power, P. (1977). Observations of eddy formation off east Australia. *J. Phys. Oceanogr.* 7, 659-669.
- Samuelsson, G., and Öquist, G. (1977). A method for studying photosynthetic capacities of unicellular algae based on *in vivo* chlorophyll fluorescence. *Physiol. Plant.* 40, 315-319.
- Sheldon, R.W., and Parsons, T.R. (1967). A continuous size spectrum for particulate matter in the sea. *J. Fish. Res. Board Can.* 24, 909-915.
- Slovacek, R.E., and Hannan, P.J. (1977). *In vivo* fluorescence determinations of phytoplankton chlorophyll *a*. *Limnol. Oceanogr.* 22, 919-925.
- Strickland, J.D.H., and Parsons, T.R. (1972). A practical handbook of seawater analysis. 2nd Edn. Fish. Res. Board Can. Bull. 167.
- Sverdrup, H.U. (1953). On conditions for the vernal blooming of phytoplankton. *J. Cons. Int. Explor. Mer* 18, 287-95.
- Turner, W.H. (1973). Photoluminescence of color filter glasses. *Applied Optics* 12, 480-486.

Table 1. 10 m interval fluorescence profiles obtained with Variosens at designated Stations¹. SP12/78. Values in Variosens units (VU).

Depth	Station							
	1	2	3	4	6	7	8	9
0	.117	.131	.108	.651	.201	.055	.043	.145
10	.138	.125	.117	.605	.210	.058	.051	.145
20	.181	.125	.131	.880	.230	.066	.055	.165
30	.181	.201	.138	.748	.152	.070	.078	.165
40	.165	.230	.125	.748	.191	.074	.108	.191
50	.191	.220	.125	.605	.220	.074	.099	.145
60	.172	.230	.125	.700	.191	.050	.099	.172
70	.191	.220	.131	.880	.131	.050	.125	.152
80	.191	.230	.145	.880	.063	.050	.108	.108
90	.165	.260	.108	.300	.066	.055	.125	.099
100	.036	.045	.099	.046	.051	.041	.070	.117
\int_0^{100}	17.	19.	12.	67.	16.	6.	9.	15.

¹ For station positions see Fig. 7.

Table 2. Percent of total protoplankton biomass represented by diatoms, flagellates, dinoflagellates, aplanospores and ciliates in surface samples at Stations 9-13. SP12/78. The Table shows that eddy stations (such as 8-11) generally had a greater proportion of flagellates than stations outside the eddies (such as 1, 4 and 13).

Station	Biomass ($\mu\text{g l}^{-1}$)	Diatoms %	Flagellates %	Dinoflagellates %	Aplanospores %	Ciliates %
1	64	76	16	4	3	1
3	22	13	32	16	9	29
4	1310	83	5	3	4	6
6	34 ¹	50	33	7	7	3
7	20	11	39	20	14	17
8	15	10	73	0	11	6
9	25	20	52	10	0	18
10	14	3	85	2	0	10
11	22	1	84	9	0	6
12	74	1	43	19	7	29
13	259	65	12	10	4	9

¹ The biomass estimate is unreliable because of leakage in the counting chamber. The bias is toward the reported figure being too small. The composition values are considered to be reliable.

Table 3. Comparison of biomass and "taxonomic units" (genera and size/shape) among surface samples from Stations 9-13. SP12/78.

Station	Biomass ($\mu\text{g l}^{-1}$)	Taxonomic units				
		Total	Diatoms	Flagellates	Dinoflagellates	Ciliates
1	64	214	169	14	27(9) ²	4
3	22	82	17	21	33(11)	11
4	1310	189	110	23	47(17)	9
6	34 ¹	133	71	25	32(15)	5
7	20	91	27	19	36(10)	9
8	15	38	5	12	16(13)	5
9	25	52	21	18	3(0)	10
10	14	27	5	14	4(0)	4
11	22	51	8	23	17(0)	3
12	74	111	16	20	62(13)	13
13	259	163	91	12	45(15)	15

¹ The biomass estimate is unreliable because of leakage in the counting chamber. The bias is toward the reported figure being too small. The composition values are considered to be reliable.

² Numbers in parentheses are for taxonomic units arising from aplanospores which are included as dinoflagellates.

Appendix 1. Protoplankton biomass estimated from micromerements grouped by Sheldon-Parsons size groups and broad taxa. SP12/78 Stn 1, surface sample.

Nominal diameter (μ)	Diatoms ($\mu\text{g } \ell^{-1}$)	Flagellates ($\mu\text{g } \ell^{-1}$)	Dinoflagellates ($\mu\text{g } \ell^{-1}$)	Aplanospores ($\mu\text{g } \ell^{-1}$)	Ciliates ($\mu\text{g } \ell^{-1}$)
5.04	0	0	0	0	0
6.34	0	1.953	0	0	0
8.00	.164	.281	0	0	0
10.1	.160	0	.234	0	0
12.7	1.164	4.492	.171	0	0
16.0	2.770	.594	.604	0	0
20.2	1.303	2.696	.079	.097	.285
25.4	4.643	.411	.098	.195	0
32.0	7.941	.206	.433	.211	.081
40.3	6.544	0	.350	0	0
50.8	16.447	0	.672	1.381	.424
64.0	5.387	0	0	0	0
80.6	3.220	0	0	0	0
102.	2.121	0	0	0	0
128.	0	0	0	0	0
Σ	51.864	10.633	2.641	1.884	.791
% Σ	76.5	15.7	3.9	2.8	1.2
N ℓ^{-1}	10 200	43 219	2 210	155	184
% Σ	18.2	77.2	3.9	0.3	0.3
average size (μ^3)	5 045	246	1 195	12 155	4 299

Appendix 2. Protoplankton biomass estimated from micromerements grouped by Sheldon-Parsons size groups and broad taxa. SP12/78 Stn 3, surface sample.

Nominal diameter (μ)	Diatoms ($\mu\text{g } \ell^{-1}$)	Flagellates ($\mu\text{g } \ell^{-1}$)	Dinoflagellates ($\mu\text{g } \ell^{-1}$)	Aplanospores ($\mu\text{g } \ell^{-1}$)	Ciliates ($\mu\text{g } \ell^{-1}$)
5.04	0	0	0	0	0
6.34	0	1.063	0	0	0
8.00	0	.177	0	0	0
10.1	.003	0	.193	0	0
12.7	.060	2.661	.367	.149	0
16.0	.026	.897	.616	.287	0
20.2	.036	1.572	.226	.094	.203
25.4	.190	.220	.349	.327	.105
32.0	.115	.085	.159	.343	.688
40.3	.332	.330	.745	.735	1.479
50.8	0	0	.560	0	0
64.0	.641	0	.358	0	.327
80.6	1.522	0	0	0	.848
102.	0	0	0	0	2.694
128.	0	0	0	0	0
Σ	2.925	7.005	3.573	1.935	6.344
% Σ	13.4	32.2	16.4	8.9	29.1
N ℓ^{-1}	287	24 834	1 863	748	310
% Σ	1.0	88.6	6.6	2.7	1.1
average size (μ^3)	10 199	282	1 917	2 587	20 465

Appendix 3. Protoplankton biomass estimated from micromerements grouped by Sheldon-Parsons size groups and broad taxa. SP12/78 Stn 4, surface sample.

Nominal diameter (μ)	Diatoms ($\mu\text{g l}^{-1}$)	Flagellates ($\mu\text{g l}^{-1}$)	Dinoflagellates ($\mu\text{g l}^{-1}$)	Aplanospores ($\mu\text{g l}^{-1}$)	Ciliates ($\mu\text{g l}^{-1}$)
5.04	0	0	0	0	0
6.34	0	6.047	.045	0	0
8.00	.483	2.368	0	0	0
10.1	9.318	.227	1.134	0	0
12.7	43.082	16.182	1.147	0	0
16.0	94.889	9.374	4.623	2.987	0
20.2	169.295	13.736	2.321	1.980	3.191
25.4	80.171	3.991	6.934	6.040	.855
32.0	161.228	3.464	2.909	6.716	2.888
40.3	159.280	1.528	6.333	9.703	7.638
50.8	163.927	0	11.405	2.280	0
64.0	72.602	4.454	0	5.345	12.515
80.6	66.898	0	0	16.182	0
102.	68.184	0	0	0	0
128.	0	0	0	0	44.651
Σ	1089.357	61.370	36.851	51.233	71.738
% Σ	83.1	4.7	2.8	3.9	5.5
N l^{-1}	353 202	164 752	17 579	5 890	2 829
% Σ	64.9	30.3	3.2	1.1	0.5
average size (μ^3)	3 084	372	2 096	8 698	25 358

Appendix 4. Protoplankton biomass¹ estimated from micromerements grouped by Sheldon-Parsons size groups and broad taxa. SP12/78 Stn 6, surface sample.

Nominal diameter (μ)	Diatoms ($\mu\text{g l}^{-1}$)	Flagellates ($\mu\text{g l}^{-1}$)	Dinoflagellates ($\mu\text{g l}^{-1}$)	Aplanospores ($\mu\text{g l}^{-1}$)	Ciliates ($\mu\text{g l}^{-1}$)
5.04	0	0	0	0	0
6.34	.000	3.330	.008	0	0
8.00	.041	.824	0	0	0
10.1	.038	.201	.117	0	0
12.7	.296	.599	0	0	0
16.0	1.579	1.740	.556	.050	0
20.2	2.437	3.028	.208	.245	.027
25.4	3.555	.684	.469	.520	.084
32.0	3.870	.315	0	.223	.466
40.3	.921	.460	.495	1.398	.283
50.8	0	0	.619	0	0
64.0	4.495	0	0	0	0
80.6	0	0	0	0	0
102.	0	0	0	0	0
128.	0	0	0	0	0
Σ	17.032	11.182	2.472	2.436	.860
% Σ	50.1	32.9	7.3	7.2	2.5
N l^{-1}	5 039	64 140	1 704	395	105
% Σ	7.1	89.9	2.4	0.6	0.1
average size (μ^3)	3 434	174	1 451	6 165	8 190

¹ Biomass estimates are not quantitative in this sample because of leakage in the counting chamber. The values are considered to be relative within the sample.

Appendix 5. Protoplankton biomass estimated from micromerements grouped by Sheldon-Parsons size groups and broad taxa. SP12/78 Stn 7, surface sample.

Nominal diameter (μ)	Diatoms ($\mu\text{g l}^{-1}$)	Flagellates ($\mu\text{g l}^{-1}$)	Dinoflagellates ($\mu\text{g l}^{-1}$)	Aplanospores ($\mu\text{g l}^{-1}$)	Ciliates ($\mu\text{g l}^{-1}$)
5.04	0	0	0	0	0
6.34	0	1.653	0	0	0
8.00	.010	.164	.089	0	0
10.1	.031	0	.099	0	0
12.7	.006	2.215	.222	0	0
16.0	.034	.611	.113	0	0
20.2	.238	1.363	.539	.583	.066
25.4	.241	.803	.358	.751	.250
32.0	.036	.323	.233	.277	.489
40.3	.066	.452	2.009	.901	2.512
50.8	.153	0	.182	.182	0
64.0	1.294	0	0	0	0
80.6	0	0	0	0	0
102.	0	0	0	0	0
128.	0	0	0	0	0
Σ	2.110	7.584	3.844	2.694	3.317
% Σ	10.8	38.8	19.7	13.8	17.0
$N \text{ l}^{-1}$	423	32 680	2 188	616	299
% Σ	1.2	90.2	6.0	1.7	0.8
average size (μ^3)	4 988	232	1 757	4 372	11 094

Appendix 6. Protoplankton biomass estimated from micromerements grouped by Sheldon-Parsons size groups and broad taxa. SP12/78 Stn 8, surface sample.

Nominal diameter (μ)	Diatoms ($\mu\text{g l}^{-1}$)	Flagellates ($\mu\text{g l}^{-1}$)	Dinoflagellates ($\mu\text{g l}^{-1}$)	Aplanospores ($\mu\text{g l}^{-1}$)	Ciliates ($\mu\text{g l}^{-1}$)
5.04	0	0	0	0	0
6.34	0	3.371	0	0	0
8.00	0	.516	0	0	0
10.1	0	0	0	0	0
12.7	0	2.427	0	0	0
16.0	0	1.820	0	.007	0
20.2	0	2.063	.009	.470	.566
25.4	.080	.071	.058	.117	.029
32.0	0	.117	0	.334	.040
40.3	0	.564	0	.652	.077
50.8	.138	0	0	0	.163
64.0	.724	0	0	0	0
80.6	.552	0	0	0	0
102.	0	0	0	0	0
128.	0	0	0	0	0
Σ	1.494	10.949	.067	1.580	.875
% Σ	10.0	73.2	0.4	10.6	5.9
$N \text{ l}^{-1}$	39	64 087	20	380	277
% Σ	0.0	98.9	0.0	0.6	0.4
average size (μ^3)	38 307	171	3 350	4 161	3 162

Appendix 7. Protoplankton biomass estimated from micromeasurements grouped by Sheldon-Parsons size groups and broad taxa. SP12/78 Stn 9, surface sample.

Nominal diameter (μ)	Diatoms ($\mu\text{g l}^{-1}$)	Flagellates ($\mu\text{g l}^{-1}$)	Dinoflagellates ($\mu\text{g l}^{-1}$)	Aplanospores ($\mu\text{g l}^{-1}$)	Ciliates ($\mu\text{g l}^{-1}$)
5.04	0	0	0	0	0
6.34	0	0	0	0	0
8.00	0	5.674	0	0	0
10.1	.002	0	0	0	0
12.7	.014	3.089	0	0	0
16.0	0	1.240	1.401	0	1.702
20.2	.060	1.451	0	0	.383
25.4	.346	.596	0	0	.736
32.0	.444	.093	0	0	.589
40.3	2.083	.234	0	0	.414
50.8	1.346	.574	.436	0	0
64.0	.617	0	0	0	.646
80.6	0	0	.728	0	0
102	0	0	0	0	0
128	0	0	0	0	0
Σ	4.912	12.951	2.565	0	4.470
$\% \Sigma$	19.7	52.0	10.3		18.0
$N \text{ l}^{-1}$	383	56 639	1 771		1 186
$\% \Sigma$	0.6	94.4	3.0		2.0
average size (μ^3)	12 830	229	1 449		3 770

Appendix 8. Protoplankton biomass estimated from micromeasurements grouped by Sheldon-Parsons size groups and broad taxa. SP12/78 Stn 10, surface sample.

Nominal diameter (μ)	Diatoms ($\mu\text{g l}^{-1}$)	Flagellates ($\mu\text{g l}^{-1}$)	Dinoflagellates ($\mu\text{g l}^{-1}$)	Aplanospores ($\mu\text{g l}^{-1}$)	Ciliates ($\mu\text{g l}^{-1}$)
5.04	0	0	0	0	0
6.34	0	3.759	0	0	0
8.00	0	1.404	0	0	0
10.1	0	0	0	0	0
12.7	.015	.977	0	0	0
16.0	0	2.408	0	0	0
20.2	.017	2.373	.154	0	1.015
25.4	.103	.176	.084	0	.135
32.0	0	.271	0	0	.258
40.3	.307	.439	0	0	0
50.8	0	0	0	0	0
64.0	0	0	0	0	0
80.6	0	0	0	0	0
102	0	0	0	0	0
128	0	0	0	0	0
Σ	.442	11.808	.238	0	1.408
$\% \Sigma$	3.2	85.0	1.7		10.1
$N \text{ l}^{-1}$	84	75 705	84		637
$\% \Sigma$	0.1	98.9	0.1		.8
average size (μ^3)	5 250	156	2 833		2 210

Appendix 9. Protoplankton biomass estimated from micromerements grouped by Sheldon-Parsons size groups and broad taxa. SP12/78 Stn 11, surface sample.

Nominal diameter (μ)	Diatoms ($\mu\text{g } \ell^{-1}$)	Flagellates ($\mu\text{g } \ell^{-1}$)	Dinoflagellates ($\mu\text{g } \ell^{-1}$)	Aplanospores ($\mu\text{g } \ell^{-1}$)	Ciliates ($\mu\text{g } \ell^{-1}$)
5.04	0	0	.003	0	0
6.34	0	3.166	0	0	0
8.00	0	1.596	0	0	0
10.1	.002	.047	0		0
12.7	.016	6.646	.006	0	0
16.0	0	1.573	1.177	0	0
20.2	.046	4.186	.278	0	0
25.4	.021	.239	.021	0	0
32.0	.057	.599	.428	0	0
40.3	.086	.496	.063	0	.353
50.8	0	0	0	0	0
64.0	0	0	0	0	0
80.6	0	0	0	0	.898
102	0	0	0	0	0
128	0	0	0	0	0
Σ	.228	18.548	1.975	0	1.251
% Σ	1.0	84.3	8.9		5.7
N ℓ^{-1}	75	79 337	1 508		45
% Σ	0.1	98.0	1.9		0.0
average size (μ^3)	3 040	234	1 310		2 780

Appendix 10. Protoplankton biomass estimated from micromerements grouped by Sheldon-Parsons size groups and broad taxa. SP12/78 Stn 12, surface sample.

Nominal diameter (μ)	Diatoms ($\mu\text{g } \ell^{-1}$)	Flagellates ($\mu\text{g } \ell^{-1}$)	Dinoflagellates ($\mu\text{g } \ell^{-1}$)	Aplanospores ($\mu\text{g } \ell^{-1}$)	Ciliates ($\mu\text{g } \ell^{-1}$)
5.04	0	0	0	0	0
6.34	0	4.944	0	0	0
8.00	.005	1.535	0	0	0
10.1	.061	0	.445	0	0
12.7	.002	8.899	0	0	0
16.0	.005	5.911	5.666	0	0
20.2	.454	8.096	3.372	.047	2.002
25.4	.293	1.036	.802	.989	2.568
32.0	0	1.021	1.529	2.336	5.191
40.3	.074	.437	1.448	1.602	2.808
50.8	0	0	.459	0	8.747
64.0	0	0	.398	.436	0
80.6	0	0	0	0	0
102	0	0	0	0	0
128	0	0	0	0	0
Σ	894	31.879	14.119	5.410	21.316
% Σ	1.2	43.3	19.2	7.3	29.0
N ℓ^{-1}	564	118 028	9 496	660	2 878
% Σ	0.4	89.7	7.2	0.5	2.2
average size (μ^3)	1 583	270	1 487	8 197	7 407

Appendix 11. Proto plankton biomass estimated from micromerements grouped by Sheldon-Parsons size groups and broad taxa. SP12/78 Stn 13, surface sample.

Nominal diameter (μ)	Diatoms ($\mu\text{g } \ell^{-1}$)	Flagellates ($\mu\text{g } \ell^{-1}$)	Dinoflagellates ($\mu\text{g } \ell^{-1}$)	Aplanospores ($\mu\text{g } \ell^{-1}$)	Ciliates ($\mu\text{g } \ell^{-1}$)
5.04	0	0	0	0	0
6.34	0	5.447	0	0	0
8.00	.449	0	0	0	0
10.1	1.661	2.655	0	0	0
12.7	.650	7.516	.048	0	.436
16.0	39.934	3.431	5.549	0	0
20.2	3.496	10.261	3.470	.165	1.838
25.4	33.049	1.348	2.918	.143	.120
32.0	22.376	.224	1.904	3.921	1.973
40.3	30.155	.807	2.357	2.136	4.571
50.8	15.184	.355	3.557	3.249	.448
64.0	16.221	0	.824	1.356	1.076
80.6	4.540	0	6.457	0	1.614
102	0	0	0	0	3.826
128.	0	0	0	0	6.457
Σ	167.715	32.044	27.084	10.971	22.359
% Σ	64.5	12.3	10.4	4.2	8.6
N ℓ^{-1}	63 942	120 272	9 121	1 270	2 486
% Σ	32.4	61.0	4.6	0.6	1.3
average size (μ^3)	2 623	267	2 830	8 638	8 994

CSIRO
Division of Fisheries and Oceanography

HEADQUARTERS

202 Nicholson Parade, Cronulla, NSW

P.O. Box 21, Cronulla, NSW 2230

NORTHEASTERN REGIONAL LABORATORY

233 Middle Street, Cleveland, Qld

P.O. Box 120, Cleveland, Qld 4163

WESTERN REGIONAL LABORATORY

Leach Street, Marmion, WA 6020

P.O. Box 20, North Beach, WA 6020